PCT

INTERNATIONAL APPLICATION PUBLISHED UNDER THE PATENT COOPERATION TREATY (PCT)

(54) Title: TRANSESOPHAGEAL MAGNETIC RESONANCE ANALYSIS METHOD AND APPARATUS
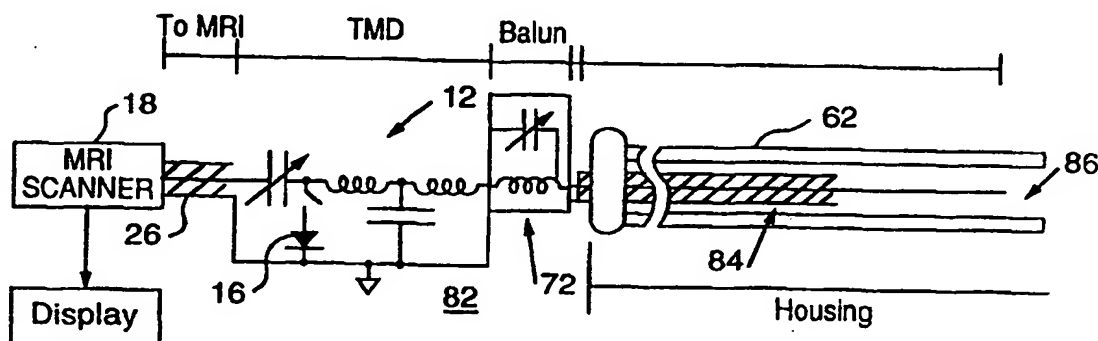
(57) Abstract

A method of trans–esophageal magnetic resonance analysis of a patient, such as an animal or human, includes providing a non–loop antenna (84), such as a coil or solenoid coil. The non–loop antenna is received within a Levin–type gastric tube (62). The gastric tube which receives the non–loop antenna is inserted in the esophagus of the patient. A tuning, matching and de–coupling circuit (12) is electrically connected to a magnetic resonance imaging scanner (18). The magnetic resonance imaging scanner (18) is employed to provide magnetic resonance imaging or spectroscopic analysis of an intra–Thoracic structure, such as the aorta, of the patient.

TRANSESOPHAGEAL MAGNETIC RESONANCE ANALYSIS METHOD AND APPARATUS

5   CROSS REFERENCE TO RELATED APPLICATION

This application claims the benefit of U.S. Provisional Application Serial No. 60/106,772, filed November 3, 1998.

BACKGROUND OF THE INVENTION

1.   Field of the Invention

10   The invention is directed to methods of magnetic resonance analysis and, in particular, to such methods for magnetic resonance imaging and spectroscopic analysis of intra thoracic anatomic structures, such as the aorta, from the esophagus of a patient. The invention is also related to a magnetic resonance analysis apparatus.

2.   Description of the Prior Art

15   Current standard techniques for imaging the thoracic aorta include X-ray computed tomography (CT), standard magnetic resonance imaging (MRI) (*e.g.*, body-coil MRI), transesophageal echocardiography (TEE), and contrast aortography. Each of these techniques suffers some important limitation in its ability to allow detailed mapping of the aortic wall and its anatomic and functional lesions.

20   Standard MRI and CT lack adequate resolution of the aortic wall for precise characterization of aortic atheromata *in vivo*, and are not able to provide measurements of focal variations in vessel wall compliance or distensibility (*e.g.*, aortic wall tissue tagging information).

TEE allows real time imaging, but suffers from both an inability to image
25   clearly that portion of the aortic wall which is directly against the esophagus due to the near field effect of ultrasound (*e.g.*, portions of the thoracic aortic wall, particularly in the arch), and from an inability to register images to a fixed frame of reference, making precise mapping of aortic lesions problematic. Kasprzak, J.D., et al., Three-dimensional echocardiography of the thoracic aorta, *Eur. Heart. J.*, vol. 17, pp. 1584-92, 1996,
30   discloses an attempt to circumvent this limitation using a technique to control movements of the probe while imaging in multiple planes with subsequent off-line 3-D image reconstruction. It is believed that the system is relatively cumbersome and not fully successful in obtaining "adequate" images in a select group of 21 patients.

Montgomery, D.H., et al., Natural history of severe atheromatous disease
35   of the thoracic aorta: a transesophageal echocardiographic study, *J. Am. Coll. Cardiol.*,

vol. 27, pp. 95-101, 1996, discloses an example of a semi-quantitative atherosclerosis grading scheme which depends upon orthogonal views to estimate the three-dimensional characteristics of aortic lesions, but does not circumvent the inherent advantage of MR over ultrasound imaging at defining atheroma structure. See, for example, Martin, A.J., et al., Arterial imaging: comparison of high-resolution US and MR imaging with histologic correlation, *Radiographics*, vol. 17, pp. 189-202, 1997.

Contrast aortography, which is often considered to provide one of the best standards for aortic imaging, is actually a misnomer since none of the tissues which make up the aortic wall are visualized directly. Instead, only lesions which protrude into the lumen and focally displace the contrast agent can be "seen" as an absence of signal. Any inferences about the vessel wall depend upon a comparison of contrast displacement from the area of the lesion to the displacement around an adjacent "reference" segment of normal artery, which is often unavailable. See, for example, Thomas, A.C., et al., Potential errors in the estimation of coronary arterial stenosis from clinical arteriography with reference to the shape of the coronary arterial lumen, *Br. Heart J., vol.* 55, pp. 144-150, 1993. It is believed that any statements about the thickness and stiffness of the vessel wall at the site of a contrast filling defect are purely conjectural.

For these reasons, some investigators prefer the term lumenography to describe standard contrast angiography in general (of which contrast aortography is a specific example). Libby, P., Lesion versus lumen, *Nature Medicine, vol.* 1, pp., 17, 18, 1995.

MRI has a distinct advantage over TEE in that tissue characterization is possible. See, for example, Toussaint, J.F., et al., Magnetic resonance images lipid, fibrous, calcified, hemorrhagic, and thrombotic components of human atherosclerosis in vivo, *Circulation,* vol. 94, pp. 932-38, 1996; and Correia, L.C.L., et al. By performing MRI using an intravascular receiver, higher resolution imaging can be achieved at the cost of invasiveness. See, for example, Ocali, O., et al.; Martin, A.J., et al., *J Magn Reson Imaging,* vol. 8, pp. 226-34; Martin, A.J., et al., *Radiographics,* vol. 17, pp. 189-202; and Atalar, E., et al., *Magn Reson Med,* vol. 36, pp. 596-605.

Intravascular MR has overcome many of the limitations of CT and standard MRI at the cost of invasiveness. Martin, A.J., et al., High-resolution MR imaging of human arteries, *J. Magn. Reson. Imaging, vol.* 5, pp. 93-100, 1995, discloses an intra-aortic catheter coil which is employed to image the aortic wall in a pig model, although the coil is relatively large and requires ligation of the aorta.

Atalar, E., et al., High resolution intravascular MRI and MRS using a catheter receiver coil, *Magn. Reson. Med.*, vol. 36, pp. 596-605, 1996, discloses a 9 French (*i.e.*, 3 mm outer diameter) catheter coil designed specifically for intravascular imaging. This validates the ability to quantitate atherosclerotic plaque burden and intraplaque composition against histopathology in cadaveric human aortae.

Although intravascular MRI is emerging as a valuable tool for studying aortic disease, *in vivo* human studies must await proper safety testing and regulatory approval.

There has been considerable interest on factors influencing atherosclerotic plaque stability. Plaque composition may predict plaque stability, and interventions that alter plaque composition may change the likelihood of plaque rupture and clinical events. Ferrari, E., et al., Atherosclerosis of the thoracic aorta and aortic debris as a marker of poor prognosis: benefit of oral anticoagulants, *J Am Coll Cardiol.*, vol. 33, pp. 1317-22, 1999, discloses that these hypotheses are supported by indirect evidence, although direct testing *in vivo* has not been possible.

The thoracic aorta represents a valuable window for the study of atherosclerotic plaque burden and vulnerability. See, for example, Fazio, G.P., et al.; Amarenco, P., et al., Atherosclerotic disease of the aortic arch and the risk of ischemic stroke, *N Engl J Med.*, vol. 331, pp. 1474-79, 1994; Cohen, A., et al., Aortic plaque morphology and vascular events: a follow-up study in patients with ischemic stroke. FAPS Investigators. French Study of Aortic Plaques in Stroke, *Circulation*, vol. 96, pp. 3838-41, 1997; and Witteman, J.C., et al., Aortic calcified plaques and cardiovascular disease (the Framingham Study), *Am J Cardiol*, vol. 66, pp. 1060-64, 1990.

The prior art also shows that atherosclerotic disease of the thoracic aorta predicts cerebrovascular events, coronary disease/events, and death.

Without invading a vascular space, it is known to obtain similar information by receiving the signal from an adjacent body structure. The concept of placing a radio frequency (RF) receiver coil into a body cavity in order to image an adjacent structure by MR is disclosed by Narayan, P., et al., Transrectal probe for 1H and 31P MR spectroscopy of the prostate gland, *Magn. Reson. Med.*, vol. 11, pp. 209-20, 1989 (an endorectal RF receiver coil is employed to image the canine prostate); and by Schnall, M.D., et al., Prostate: MR imaging with an endorectal surface coil, *Radiology*, vol. 172, pp. 570-74, 1989 (an expandable endorectal RF receiver coil is employed to

image the prostate in 15 humans having biopsy proven prostate carcinoma and two normal volunteers).

U.S. Patent No. 5,348,010 discloses a rectal MRI receiving probe for use in imaging the prostate.

It is known to employ an endovaginal coil to image the vagina and adjacent structures. See, for example, Siegelman, E.S., et al., High-resolution MR imaging of the vagina, *Radiographics,* vol. 17, pp. 1183-1203, 1997.

U.S. Patent No. 5,355,087 discloses the use of a probe in MRI or spectroscopy related to either the prostate or cervix. An RF receiving coil is inserted into the rectum or vagina in effecting these respective measurements.

It is also known to study the aorta by employing an expandable coil-type RF receiver in the inferior vena cava. See Martin, A.J., et al., An expandable intravenous RF coil for arterial wall imaging, *J. Magn. Reson. Imaging,* vol. 8, pp. 226-34, 1998. While this approach avoids the need to invade the aorta, it necessitates placement of a large caliber central venous catheter, with associated risks.

U.S. Patent No. 5,928,145 discloses magnetic resonance imaging (MRI) and spectroscopic analysis of small blood vessels using a flexible probe of relatively small dimension. A loopless antenna is employed wherein a coaxial cable is structured to be received within the intravascular system, a blood vessel such as a human vein, the femoral artery of a live rabbit for imaging the aorta thereof, a naturally occurring passageway in a human being, an opening of the pancreatic duct, or a tortuous passageway of a patient. In one embodiment, the optimal length of the antenna is about 7 cm to 10 cm and the loopless antenna has a maximum width of about 0.5 mm to 1.0 cm. Matching and decoupling circuits are employed. Preferably, the loopless antenna is flexible for purpose of movement in a tortuous path. Patent 5,928,145 does not disclose any esophageal insertion of an antenna nor any insertion of an antenna in one body passageway to image body portions external to that passageway.

U.S. Patent Application Serial No. 08/979,121 discloses the use of a body coil and support member and a catheter antenna employed for insertion into the body. An endoscope is inserted through the patient's mouth into the esophagus with an antenna in the form of a coaxial cable being delivered therethrough. The antenna is delivered to the esophagus by the endoscope which serves as a support surface therefor. Cylindrically encoded images are produced around the endoscope.

It is believed that an endoscope generally requires the sedation of the patient.

U.S. Patent No. 5,699,801 discloses a flexible receiver coil for introduction into small blood vessels for purposes of accessing atherosclerotic areas. The receiver coil is introduced into or adjacent to the specimen, such as a patient. The coil is inserted within a catheter, an endoscope, a biopsy needle, or other probe-type medical devices.

U.S. Patent No. 5,792,055 discloses the use of a coaxial cable functioning as an antenna in MRI procedures with particular emphasis on vascular uses.

U.S. Patent No. 5,432,450 is directed toward an MRI probe having internal and external conductors.

U.S. Patent No. 5,419,325 is directed to MRI and spectroscopy and discloses the use of a Faraday catheter inserted into a blood vessel of a patient.

U.S. Patent No. 5,417,713 is directed toward a defribillating system for the heart which is inserted into the esophagus.

U.S. Patent No. 5,211,166 discloses a biopsy needle or similar instrument or radiation-containing capsule, which is adapted to be detected by MRI procedures.

U.S. Patent No. 4,572,198 discloses an MRI catheter which facilitates location of the catheter tip.

U.S. Patent No. 5,170,789 discloses an insertable probe which has a two-component structure (i.e., a handle portion and an insertable portion having a coil). MRI and spectroscopy is employed to study deeply located organs, such as the rectum, colon, prostate, bladder, cervix and other tissue in close proximity to these or other internal organs.

The prior art shows that there is room for improvement in the known methods and apparatus for magnetic resonance imaging and spectroscopic analysis of the aorta and other intra thoracic anatomic structures.

SUMMARY OF THE INVENTION

As one aspect of the invention, a method of transesophageal magnetic resonance analysis of a patient comprises providing a non-loopless antenna; receiving the non-loopless antenna in a gastric tube; inserting the gastric tube which receives the non-loopless antenna in the esophagus of the patient; employing a matching and tuning circuit for the non-loopless antenna external to the patient; electrically connecting the matching

and tuning circuit to a magnetic resonance scanner; and employing the magnetic resonance scanner for magnetic resonance imaging or spectroscopic analysis of an intra thoracic anatomic structure of the patient.

The gastric tube may be a Levin gastric tube. Preferably, the gastric tube is employed as a nasogastric tube, and transnasal placement of the nasogastric tube is employed in the esophagus of the patient.

As another refinement, the non-loopless antenna may be employed to confirm proper placement of the gastric tube in the esophagus of the patient.

As another aspect of the invention, a transesophageal magnetic resonance analysis apparatus for a patient comprises a non-loopless antenna; a gastric tube for receiving the non-loopless antenna and for inserting the non-loopless antenna in the esophagus of the patient; a matching and tuning circuit having a first port and a second port which is electrically connected to the non-loopless antenna; magnetic resonance scanner means for magnetic resonance imaging or spectroscopic analysis of an intra thoracic anatomic structure of the patient; and a cable electrically connecting the first port of the matching and tuning circuit to the magnetic resonance scanner means.

These and other objects of the present invention will be more fully understood from the following description of the invention with reference to the illustration appended hereto.

BRIEF DESCRIPTION OF THE DRAWINGS

Figure 1A is an isometric view of a transesophageal magnetic resonance imaging (TEMRI) device in accordance with the invention;

Figure 1B is a schematic diagram of the TEMRI device of Figure 1A;

Figure 2A is a representation of a transesophageal magnetic resonance tissue-tagged slice image;

Figure 2B is a representation of a transesophageal magnetic resonance tissue-tagged transverse image;

Figure 2C is a representation of a transesophageal magnetic resonance tissue-tagged longitudinal image;

Figures 3A-3D are representations of transesophageal magnetic resonance images of the aorta of a rabbit;

Figure 4 is a representation of a standard body coil magnetic resonance image of a rabbit with the TEMRI device of Figure 1A in position in the esophagus;

Figure 5A is an isometric view of a TEMRI antenna and gastric tube in accordance with another embodiment of the invention;

Figure 5B is a plan view of a transesophageal echocardiography (TEE) probe, a 12 French (*i.e.,* 4 mm outer diameter) gastric tube and an 8 French (*i.e.,* 2.67 mm outer diameter) gastric tube;

Figure 5C is a schematic diagram of a TEMRI device which includes the TEMRI antenna and gastric tube of Figure 5A;

Figure 6A is a representation of an image of the descending thoracic aorta of a healthy human, obtained from the TEMRI device of Figure 5A in position in the esophagus;

Figure 6B is a representation of an image of the descending thoracic aorta of the human from Figure 6A, obtained from an MRI coil on the patient's back;

Figure 6C is a representation of an image of a descending thoracic human aorta in which there is diffuse thickening with a smooth surface contour and without plaque tissue heterogeneity, obtained from the TEMRI device of Figure 5A in position in the esophagus;

Figure 6D is a representation of an image of the distal aortic arch of an elderly human having a remote stroke, obtained from the TEMRI device of Figure 5A in position in the esophagus;

Figure 6E is a representation of an image of the distal aortic arch of the human of Figure 6D, obtained from a TEE probe in position in the esophagus;

Figure 6F is a plot of the relationship between measured circumferential extent of $\geq$2.0 mm aortic wall thickening assessed by TEE (y-axis) with respect to TEMRI (x-axis); and

Figure 7 is a schematic diagram of a TEMRI device in accordance with another embodiment of the invention which device includes a non-loopless antenna and a gastric tube.

DESCRIPTION OF THE PREFERRED EMBODIMENTS

As employed herein, the term "loopless antenna" shall expressly include, but not be limited to, a dipole antenna and any and all equivalents thereof, such as, for example, a dipole antenna having two poles at least one of which includes a mechanical loop (see, *e.g.,* Figure 14 of Patent 5,928,145).

As employed herein, the term "antenna" shall expressly include a loopless antenna and any other imaging or spectroscopic analysis antenna, coil (*i.e.,* having one turn)

or solenoid coil (*i.e.*, having plural turns) which may be received by a gastric tube and which may receive an RF signal of appropriate frequency.

As employed herein, the term "non-loopless antenna" shall expressly include any antenna, other than a loopless antenna, which may be received by a gastric tube and which may receive an RF signal of appropriate frequency.

As employed herein, the term "patient" shall mean human beings and other members of the animal kingdom.

Referring to Figure 1A, a loopless RF receiver device in the form of the exemplary transesophageal MR imaging (TEMRI) device 2 is shown. The TEMRI device 2 is designed for ease of placement into the esophagus of a patient for imaging of the adjacent aorta. Also referring to Figure 1B, the exemplary device 2 includes a loopless RF receiver antenna 4 constructed from a flexible 0.047 inch diameter 50 Ω coaxial cable 6, with a 10 cm extension 8 of the center conductor at the distal end. The antenna 4 is secured within a modified Levin-type gastric tube 10. A tuning, matching and decoupling (TMD) circuit 12 is enclosed in an exemplary aluminum box 14. Although an aluminum box is disclosed, any non-ferromagnetic enclosure (*e.g.*, copper) may be employed. The coaxial cable 6 is connected to the TMD circuit 12 which lies outside the patient's body. Decoupling is provided by high-speed diode switching of diode 16 during external RF pulses from a suitable MRI scanner 18. This prevents the antenna 4 from receiving during external RF pulses, yet allows signal reception between pulses. In the exemplary embodiment, the housing of the gastric tube 10 is 12 French in diameter, although other sizes are possible.

The present invention exploits the proximity of the esophagus and the descending thoracic aorta, which are directly juxtaposed throughout the length of the descending thoracic aorta. By employing the gastric tube 10, the loopless RF antenna 4 may be passed down the esophagus of a non-sedated patient, such as a human or another suitably large animal. In turn, the antenna 4 provides information comparable to that obtained with intravascular MRI and not obtainable by other non-invasive methods.

Example 1

The exemplary transesophageal MRI (TEMRI) antenna 4 is based upon the design and construction of the MRI-compatible loopless RF receiver antenna disclosed in Patent 5,928,145; and Ocali, O., et al., Intravascular magnetic resonance imaging using a loopless catheter antenna, *Magn. Reson. Med.*, vol. 37, pp. 112-18, 1997,

except that the antenna 4 is designed to fit and operate inside a modified Levin gastric tube 10 (e.g., marketed by Sherwood Medical, St. Louis, Missouri). Exemplary sizes of the gastric tube 10 include 8 French (e.g., suitable for rabbit studies) or 12 French (e.g., suitable for obtaining images in mini-swine) as shown in Figure 1A. The prior intravascular loopless catheter antenna has been used for *in vivo* intravascular imaging of rabbit aortae. See, for example, Patent 5,928,145; Ocali, O., et al.

The exemplary TEMRI device 2 consists of a relatively thin coaxial cable 6 which is ≈λ/4 in length and which has a 10 cm extension 8 of the inner conductor at the distal end. The distal portion of the antenna 4 is housed inside the Levin gastric tube 10, which is modified by being suitably cut to adjust its length and being suitably marked (e.g., at 20 of Figure 1A) to assist in proper esophageal placement. The proximal end 22 of the antenna 4 protrudes from the proximal end 24 of the Levin tube 10 at which point the two are secured together to prevent the antenna 4 from migrating out the end of the Levin tube housing 10. The proximal end 22 of the antenna 4 is connected to the adjustable TMD circuit 12, which, in turn, is connected via a coaxial cable 26 to the MRI scanner 18, such as a GE 1.5 Tesla MRI system.

As a further example, the exemplary TEMRI antenna may be employed in animals, such as a mini-swine (e.g., 35-45 kg) and a New Zealand white rabbit (e.g., ≈ 5 kg). Preferably, the animals are handled to ensure compliance with all relevant Federal regulations.

Transnasal esophageal placement of the TEMRI device 2 is confirmed, for example, by fluoroscopy in the case of the mini-swine. Tagged and non-tagged cine images are obtained in the manner disclosed in McVeigh, E.R., et al., Cardiac tagging with breath-hold cine MRI. *Magn. Reson. Med.,* vol. 28, pp. 318-27, 1992; and Zerhouni, E.A., et al., Human heart: tagging with MR imaging—a method for noninvasive assessment of myocardial motion, *Radiology,* vol. 169, pp. 59-63, 1988. Exemplary imaging parameters are discussed, below, in connection with Figures 2A-2C, and 3A-3D.

Figures 2A-2C represent images of the thoracic aorta 27 obtained by the TEMRI antenna device 2 of Figures 1A-1B in the esophagus 28 of a living, anesthetized mini-pig. Adjusting the imaging parameters of the MRI scanner 18 of Figure 1B allows differentiation of the aortic wall from both surrounding tissues and intra-aortic blood. Images may be obtained with tissue-tagging, as in Zerhouni, E.A., et al., and ECG-gating

at five frames per cardiac cycle, in order to demonstrate focal movement of the aortic wall in response to pulsatile blood flow, which reflects focal stress/strain relationships.

Exemplary imaging parameters common to Figures 2A-2C include: ECG-gated, segmented k-space, SPGR with HOT pulses (see, for example, Atalar, E., et al., Minimization of dead-periods in MRI pulse sequences for imaging oblique planes, *Magn. Reson. Med.*, vol. 32, pp. 773-77, 1994) at 10 cm FOV, 256 x 140 matrix, and flip = 15°.

The image represented by Figure 2A was obtained without tissue tagging. A short axis 7 mm slice was obtained 7.7 cm proximal to the probe tip, during a 27 s breath-hold, with number of excitations (NEX) 4, TR / echo time (TE) 7.7/2.2 ms, and 44 ms delay from QRS.

Tissue-tagged images were obtained with ECG-gating at 5 frames per cardiac cycle to allow direct visualization of aortic wall strain in response to pulsatile blood flow. Figures 2B and 2C represent 159 ms delay images from tissue tagged, ECG-gated cine-loops obtained at 44, 83, 121, 159, and 198 ms after detection of the QRS complex. Those images are transverse and longitudinal images, respectively, which were obtained using tissue tagging which appears as transverse lines of voided signal. The particular imaging parameters for Figure 2B include: 7 mm thick, 7.7 cm proximal to the probe tip, during a 10 s breath-hold, with NEX 2, TR/TE 7.7/2.2 ms, and 159 ms delay from QRS. For Figure 2C, the imaging parameters include: 3 mm thick, during a 28 s breath-hold, with NEX 6, TR/TE 8.7/2.6 ms, and 159 ms delay from QRS.

As shown in Figures 2A-2C, the location of the TEMRI probe 2 in each image representation is recognized by the characteristic appearance (Figure 2B) of a small dark region reflecting the actual silver and copper coaxial RF receiver within the brightest region of the image. In some cases, a target appearance of the probe is evident. It is believed that this represents the (dark) metallic conductor 30 in the center, surrounded by gastric fluid (bright) 32, surrounded by plastic (dark) 34 from the modified Levin tube probe housing, all within the brightest region of the image. In practical terms, recognizing the location of the probe within the image is not difficult.

Referring to Figures 3A-3D, the TEMRI technique is also applied to a relatively smaller animal. An 8 French version (see the corresponding housing 68 of Figure 5B) of the TEMRI antenna is easily passed transnasally into the esophagus 36 of a living anesthetized rabbit. This allows imaging of the rabbit aorta 38, including the aortic wall 40, which is ≈ 0.2 mm thick. Representations of ECG-gated TEMRI images from the rabbit are obtained with a 61 ms delay from the detection of the QRS complex.

Exemplary imaging parameters include: fast spin echo at 8 cm FOV, 256 x 256 matrix, and flip = 15°.

Figure 3A is a representation of an image in the form of a 3 mm longitudinal slice through the aorta 38 from the arch 42 to well below the diaphragm 44. Exemplary imaging parameters include: single breath-hold, NEX 8, and TR/TE 600/19.6 ms.

Figures 3B, 3C and 3D are representations of images in the form of 3 mm short axis slices at relatively high, middle, and low positions within the descending thoracic aorta 38 (e.g., 7.8 cm, 5.4 cm, and 4.6 cm from the distal tip of the probe, respectively). In Figures 3B and 3C, the aortic wall 40 separates lung 46 and aortic blood 48. This demonstrates that the TEMRI technique can resolve the aortic wall 40, which in a rabbit is ≅ 0.2 mm thick. In Figure 3D, the TEMRI antenna device 50 is shown in the esophagus 36 at the gastroesophageal junction 52. Exemplary imaging parameters for these images include: single breath-hold, NEX 8, and TR/TE 600/11.8 ms.

The sensitivity of the exemplary TEMRI antenna decreases with the longitudinal distance from its receptive center and linearly with radial distance from the antenna, Ocali, O., et al., but is maintained at a reasonable level over a useful range. This is seen qualitatively as the brightness of the image representations in both their longitudinal and radial dimensions.

For applications in which the relative values of the signal intensities at two different locations are important, the image may be corrected after acquisition using a suitable algorithm in the MRI scanner which accounts for this property of the antenna.

Example 2

Referring to Figure 4, standard MR (body coil) imaging may be employed while the TEMRI device 54 is in the esophagus 56. Figure 4 shows a representation of the MR image of a rabbit 58 with the TEMRI device 54 in position in the esophagus 56. While the TEMRI device 54 was in place in the esophagus 56, standard MRI was performed. The exemplary imaging parameters in connection with Figure 4 include: ECG-gated, fast spin echo at 28 cm FOV, 256 x 256 matrix, 3 mm thick, single breath hold, NEX 2, and TR 2000. The presence of the TEMRI device 54 in the esophagus 56 did not interfere with the standard MR imaging, which can be used to confirm proper

placement in the distal esophagus 59. Hence, this technique may be employed to verify proper position of the TEMRI device 54 within the distal esophagus 59.

As discussed above, TEMRI may be applied to the study of the thoracic aorta. This technique may also have application to studies of aortic atheroma size, morphology and composition. While these properties have previously been studied *ex vivo* and by intravascular MR (see, *e.g.*, Martin, A.J., et al., *Radiographics,* vol.17, pp. 189-202; Martin, A.J., et al., *J. Magn. Reson. Imaging,* vol. 5, pp. 93-100; Toussant, J.F., et al., Water diffusion properties of human atherosclerosis and thrombosis measured by pulse field gradient nuclear magnetic resonance, *Arterioscler. Thromb. Vasc. Biol.,* vol. 17, pp. 542-46, 1997; Toussant, J.F., et al., Magnetic resonance images lipid, fibrous, calcified, hemorrhagic, and thrombotic components of human atherosclerosis in vivo, *Circulation.,* vol. 94, pp. 932-38, 1996; Correia, C.L., et al; Toussant. J.F., T2-weighted contrast for NMR characterization of human atherosclerosis, *Arterioscler. Thromb. Vasc. Biol.,* vol. 15, pp. 1533-42, 1995), such properties cannot be measured as well by competing non-invasive techniques.

The exemplary TEMRI loopless antenna 4 of Figure 1B has several advantages over other candidate TEMRI antenna designs which incorporate coils. First, while the coil design theoretically has a higher signal-to-noise ratio (SNR), this advantage only persists in the region immediately adjacent to the probe. See Atalar, E., et al.; Ocali, O., et al. In practice, a small caliber coil with a conductor separation of 1.5 mm will outperform a loopless receiver at < 1 cm from the receiver. However, beyond 1 cm, the loopless design affords a higher SNR. This is because the SNR for a receiver coil decreases with the inverse square of the distance from the coil, but the SNR for a loopless receiver decreases with the linear inverse of the distance. This linear inhomogeneity of signal from a loopless receiver is quite predictable across the field of view and can be corrected to homogeneity after image acquisition with an appropriate algorithm as described in Atalar, E., et al. In principle, this allows a quantitative comparison of signal intensity between two pixels whose distances from the probe differ. However, as is the case with most diagnostic imaging modalities, limiting post-acquisition processing of the images may be preferable.

In addition, since coil receivers require capacitor components near the distal end of the device, a larger caliber is mandated and construction is more complex. See Atalar, E., et al.; Ocali, O., et al. Expandable coils can extend the range over which a coil design outperforms a loopless receiver by increasing the diameter of the coil (see,

e.g., Schnall, M.D., et al., *Radiology,* vol. 172, pp. 570-74; Siegelman, E.S., et al.; and Martin, A.J., et al., *J. Magn. Reson. Imaging,* vol. 8, pp. 226-34), however, they add further to the complexity of device design and placement. Thus, for imaging the human aorta which is normally 2-3 cm in diameter, and which is immediately adjacent to the

5   esophagus, a loopless RF receiver sacrifices little, if anything, to the coil receiver in terms of performance, yet is simpler to construct and use.

Example 3

For use in human subjects, a suitable TEMRI antenna device includes a 1.2 mm diameter loopless antenna receiver 60 for housing by a modified 12 French

10 Levin gastric tube 62 as shown in Figure 5A. This device may be positioned in the human esophagus by a standard nasogastric tube placement technique (*e.g.*, to measure the proper position externally, mark the device, then pass it to the pre-marked level). Proper position may then be confirmed either by a rapid external body coil image, such as employed with the rabbit 58 of Figure 4, or by MRI fluoroscopy techniques (see, *e.g.*,

15 Atalar, E., et al., Catheter-tracking FOV MR fluoroscopy, *Magn. Reson. Med.,* vol. 40(6), pp. 865-72, 1998).

The advantage of a simple, relatively small caliber device, such as the loopless TEMRI device 2 of Figures 1A and 1B, lies as much in practical issues as with theoretical concerns. As shown in Figure 5B, in contrast to a TEE probe 64, a

20 nasogastric tube, such as 66,68 (*e.g.*, 12 French, 8 French, respectively) is relatively small and can be passed transnasally into proper position in the esophagus of a cooperative, conscious patient. A nickel coin ($0.05) 69 is shown for size comparison in Figures 5A and 5B.

Once the TEMRI antenna, which is housed by the nasogastric tube, is in

25 position, no further manipulation of the TEMRI device is required in order to obtain different views. The net result is a decreased requirement for highly trained technical expertise in order to place the TEMRI device and, further, there is no need for sedation of the patient. This approach also avoids the need for a large caliber central venous catheter as is required by the transvenous approach. Although a nasogastric tube is disclosed, an

30 orogastric tube may be employed. However, nasogastric placement is generally better tolerated by the patient.

Previous investigators have suggested that aortic atherosclerosis, as detected by TEE, can serve as a surrogate marker for coronary atherosclerosis. See, for

example, Matsumura, Y., et al., Atherosclerotic aortic plaque detected by transesophageal echocardiography: its significance and limitation as a marker for coronary artery disease in the elderly, *Chest,* vol. 112, pp. 81-86, 1997; Khoury, Z., et al., Frequency and distribution of atherosclerotic plaques in the thoracic aorta as determined

5   by transesophageal echocardiography in patients with coronary artery disease, *Am. J. Cardiol.,* vol. 79, pp. 23-27, 1997; and Fazio, G.P., et al., Transesophageal echocardiographically detected atherosclerotic aortic plaque is a marker for coronary artery disease, *J. Am. Coll. Cardiol.,* vol. 21, pp. 144-50, 1993.

Fazio et al. employed TEE to study a diverse group of 61 patients

10   scheduled for coronary angiography and found 95% and 82% positive and negative predictive values, respectively, for the ability of aortic atherosclerosis on TEE to predict a significant coronary lesion (*i.e.,* 70% stenosis of a major coronary artery or 50% stenosis of the left main coronary artery). In more defined populations, Matsumura, Y., et al. (the specificity was only 55% and 10% in the subgroups under or over age 70,

15   respectively), and Khoury, Z., et al. (the specificity was 77% and 40% in subgroups under or over age 64, respectively), both found 93% sensitivities of TEE for predicting the presence of $\geq$50% stenosis of a major coronary artery as determined at coronary angiography, but the specificities were poor.

Montgomery, D.H., et al. discloses TEE to follow the natural history of

20   aortic atheromatous disease. While the overall severity of atherosclerosis may not significantly change over time, individual lesions are sporadically active and have a high likelihood of worsening or regressing over time. This reinforces the current consensus view of Libby, P., that while atherosclerosis may be slowly progressive, it is so only because the sum of the activities in each individual lesion is slowly progressive. Many

25   clinical events, in fact, likely result from a single plaque catastrophe.

Other investigators have employed TEE to image aortas in patients with familial hypercholesterolemia before and after a trial of strict cholesterol-lowering therapy, using biplane TEE and semiquantitative scores of both atheroma burden and circumferential aortic wall stiffness. They have found a decrease in both after therapy.

30   See Tomochika, Y., et al., Improvement of atherosclerosis and stiffness of the thoracic descending aorta with cholesterol-lowering therapies in familial hypercholesterolemia, *Arterioscler. Thromb. Vasc. Biol.,* vol. 16, pp. 955-62, 1996.

For this important need of monitoring response to anti-atherosclerotic therapy, TEMRI has several potential advantages over TEE. First, the corresponding probe is smaller (as shown in Figure 5B) and can be passed in the same manner as a standard nasogastric tube (*i.e.*, by a well-trained nurse with neither sedation nor the additional monitoring which conscious sedation mandates). Second, MRI-based techniques more readily allow registration of images to a fixed frame of reference than does TEE, since the absolute position of each MRI slice is known and can be related to the locations of anatomic landmarks. Since TEE requires manual aiming of the ultrasound beam at an object of interest, the probe position is not a fixed point of reference. Thus, unless two referenced landmarks are visible in the same TEE field of view as an object of interest, the object's position in space cannot be determined precisely. This makes TEE an imperfect tool for monitoring the fate of a particular atherosclerotic plaque over time, particularly in areas with many plaques and few landmarks. Third, MRI provides more lesion detail and information about plaque composition. See, for example, Yuan, C., et al., In vitro and in situ magnetic resonance imaging signal features of atherosclerotic plaque-associated lipids, *Arterioscler. Thromb. Vasc. Biol., vol.* 17, pp., 1496-503, 1997. Plaque composition is a strong predictor of plaque stability and, therefore, clinical events. Finally, with the use of tissue-tagging and ECG-gated cine-loop acquisition, TEMRI potentially provides a tool for measuring focal changes in wall stiffness, which is perhaps the most sensitive indicator of pre-clinical disease or response to therapy.

TEMRI may also be employed for quantitating thoracic aortic atherosclerosis in comparison with TEE and surface-coil MRI. TEMRI is not only useful in animals, but may also be employed to image the thoracic aorta in human subjects with and without aortic atherosclerosis.

In terms of safety, the potential for heating of a TEMRI antenna device within a patient is the primary concern. Whether the energy from the currents induced in the loopless antenna is of sufficient magnitude to produce a significant local temperature increase and a subsequent thermal tissue injury depends upon the switching, or "decoupling", efficiency of the TMD circuit 12 of Figure 1B. The TMD circuit 12 is designed to turn off RF reception during external RF pulses. Intrinsic to the MRI magnet (not shown) of the MRI scanner 18 is a feature which detects a change in the bias current used to decouple the antenna 4. If the scanner 18 detects a change in this bias current, then the scanner 18 alarms that condition and shuts down the pulse sequence. For

example, this safety feature may be triggered during a deliberate attempt to operate the TEMRI device in a phantom with the decoupling disabled. However, known studies in animals and phantoms have not triggered that safety feature during the time when the decoupling feature of the TMD circuit 12 was enabled.

Furthermore, at the end of certain studies, the animal under study was sacrificed and its aorta and esophagus were harvested *en bloc* for gross and microscopic histopathologic examination by an expert pathologist for evidence of tissue injury using standard hematoxylin and eosin stains. The absence of evidence of thermal injury to either pig or rabbit esophagus during known studies appears to confirm that decoupling is efficient. Hence, this provides a preliminary indication that TEMRI is likely to be safe.

Example 4

High-resolution images of the thoracic aortic wall were obtained by TEMRI in 20 human subjects including seven normal controls and thirteen with aortic atherosclerosis. In eight subjects, the wall thickness and circumferential extent of thickening as measured by TEMRI was compared with such measurements from TEE. TEE provided a relative underestimation of circumferential extent. The SNR of TEMRI versus the SNR of surface-coil MRI were compared in different regions of the descending thoracic aortic wall, with the SNR advantage of TEMRI being better by a factor of 1.6 to 6.0. Based upon these studies, TEMRI provides superior results to those of surface-coil MRI and TEE for quantitative assessment of thoracic aortic atherosclerotic plaque burden. Furthermore, TEMRI is a feasible method of studying morphological detail within atherosclerotic plaques, without the need to invade a vascular space.

Example 5

Figure 5C is a schematic diagram of a transesophageal magnetic resonance imaging device 70. The TEMRI loopless antenna receiver 60 is connected via TMD circuit 12 and coaxial cable 26 to the MRI scanner 18. A suitable balun circuit 72 is preferably interposed between the TMD circuit 12 and the receiver 60 to block the transmission of unbalanced currents toward the receiver 60 and, thus, the patient (not shown). In theory, without the balun circuit 72, if the MRI connector cable 26 is inadvertently left in a loop configuration during scanning, then, in principle, induced currents might heat the TEMRI device 70 and, thus, cause that heat to be transmitted to

the patient. Although the exemplary TEMRI antenna device 70 is not completely sealed at the antenna end 74, a sealed TEMRI device may also be employed.

<u>Example 6</u>

The exemplary TEMRI device 70 of Figure 5C may be placed

5   transnasally into the esophagus and stomach of the human subject using topical benzocaine spray as needed. Proper positioning may be confirmed by auscultation and aspiration. For subjects who might become claustrophobic in the magnet (not shown) of the MRI scanner 18, intravenous midazolam may be administered in order to continue the study. MR imaging studies were performed with a GE 1.5T magnet, using the

10   magnet coil to transmit, and the TEMRI loopless antenna receiver 60 to receive the signal. In some cases, the TEMRI device 70 may be arrayed with a surface-coil (*e.g.*, 5 x 11 inch rectangular coil; GE FlexCoil). Specific imaging parameters are discussed below in connection with Figures 6A-6F.

The first eight subjects for whom a contemporaneous TEE was available

15   were analyzed quantitatively. A TEMRI slice through the thoracic aorta perpendicular to blood flow was analyzed from each subject using suitable software (*e.g.*, NIH Image 1.62 for Macintosh). Aortic wall thickness, excluding adventitia, was measured to determine maximum and minimum.

In addition, slices from normal subjects were measured in arbitrary

20   locations to generate a population of 84 wall thickness measurements; the mean and standard deviation (SD) were 1.03 ± 0.32 mm. A thickness of ≥ 2.0 mm (mean + 3 SDs) was defined as being abnormal. The extent of atherosclerosis was defined as the number of degrees ≥ 2.0 mm thick.

For paired TEE measurements, the resulting video was reviewed, allowing

25   forward, reverse and pause. The reviewer's time-integrated interpretation of aortic wall was traced over a calibrated transparency to determine maximum and minimum wall thickness and extent of thickening.

Representations of *in vivo* images are shown in Figures 6A, 6C and 6D of a human thoracic aorta **Ao** as obtained by a TEMRI antenna device **De** in the esophagus

30   **Es.** Imaging parameters include: a single breath, ECG-gated, fast spin echo, blood suppression, and 12 cm FOV. The length of the reference bar 76 in Figures 6A-6E is 1 cm.

Figures 6A and 6B (*i.e.*, slice thickness 3 mm, TE 40 ms, NEX 2) show the descending thoracic aorta **Ao** of a normal 24 year old female as obtained

simultaneously from TEMRI and from a GE FlexCoil on the patient's back, respectively. These demonstrate the relative SNR advantage of TEMRI.

To quantitate this SNR advantage, SNR was measured directly (*e.g.*, Constantinides, C.D., et al., Signal-to-noise measurement in magnitude imaging from NMR phased arrays, *Magn Reson Med.*, vol. 38, pp. 852-57, 1997) in images from a thin subject with aortic atherosclerosis, in order to bias the comparison against TEMRI. The distance from the receiver **De** to the aortic wall nearest the esophagus **Es** was 8.4 mm by TEMRI and 86.3 mm by surface-coil MRI. The corresponding SNRs were 124.4 and 20.5, respectively, which provided a 6-fold advantage in TEMRI. At the aortic wall furthest from the esophagus **Es**, those distances were 29.3 mm and 78.8 mm and the SNRs were 23.3 and 14.9, respectively, which provided a 1.6-fold advantage in TEMRI.

The representation of the TEE image in Figure 6E illustrates three of its important limitations for aortic plaque imaging: (1) the aortic wall is not imaged in its 360° entirety due to near field effects, resulting in underestimation of disease extent (see Figure 6F) (*e.g.*, well over one third of the aortic circumference is not adequately assessed for measurements as simple as aortic wall thickness); (2) image quality is sensitive to the quality of esophageal contact, which is often difficult to obtain at certain anatomic locations such as at the aortic arch; and (3) tissue characterization is limited. The extent to which the real-time motion feature of TEE can overcome these limitations remains subjective. For example, in comparisons, the user may employ that potential advantage of TEE by reviewing video in motion and, then, by synthesizing the visual information into a single interpretive tracing of the aortic wall.

Figure 6C represents a TEMRI image (5 mm thick, TE 10 ms, 8 NEX) of the descending thoracic aorta **Ao** of a 58 year old female with a recent transient ischemic attack (*i.e.*, "mini-stroke"). This image representation demonstrates diffuse thickening with a smooth surface contour and without plaque tissue heterogeneity.

Figures 6D and 6E represent TEMRI and TEE images (10 mm thick, TE 15 ms, 4 NEX), respectively, from the distal aortic arch of a 78 year old male with a remote stroke. These demonstrate circumferential atherosclerotic thickening with tissue heterogeneity consistent with intraplaque calcification or hemorrhage (*e.g.*, Correia, L.C.L., et al., Intravascular magnetic resonance imaging of aortic atherosclerotic plaque composition, *Arterioscler. Thromb. Vasc. Biol.*, vol. 17, pp. 3626-32, 1997).

TEMRI was compared to TEE for quantitative assessment of atherosclerosis in the thoracic aorta. The maximum and minimum wall thicknesses were

3.5 ± 1.2 mm and 1.2 ± 0.8 mm, respectively, by TEE; and 3.3 ± 1.5 mm and 1.0 ± 0.7 mm, respectively, by TEMRI. Similarly, the circumferential extent of atherosclerosis was measured by both techniques. As shown in Figure 6F, the relationship between measured circumferential extent of ≥ 2.0 mm aortic wall thickening (degrees) assessed

5   by TEE (y-axis) is plotted with respect to TEMRI (x-axis). The identity line 78 and the best-fit line 80 through the data points are shown. While the exemplary correlation is good (i.e., r=0.84, p=0.019), relative underestimation of the extent of disease by TEE was reflected by the slope (i.e., 0.387) of the best-fit line through paired measurements.

The feasibility of high-resolution MRI of the thoracic aortic wall and its

10   atherosclerotic lesions has been demonstrated in human subjects in vivo by TEMRI. TEMRI provides a higher SNR than does surface-coil MRI. TEMRI also provides more complete information and morphologic detail within atherosclerotic plaques than does TEE. The exemplary loopless antenna design provides an imaging range well suited for imaging the aorta from the esophagus. In contrast to a TEE probe, the TEMRI probe is

15   relatively small and can be passed transnasally in an unsedated patient. Once the device is positioned, multiple views can be obtained without further manipulation. Because sedation is not required, the need for additional nursing monitoring and for the presence of a highly trained operator during imaging may prove unnecessary.

Despite its limitations, TEE provides useful information about the aortic

20   wall which likely mirrors the coronaries. See Witteman, J.C., et al., Am J Cardiol, vol. 66, pp. 1060-64. Montgomery, D.H., et al., J Am Coll Cardiol., vol. 27, pp. 95-101, follows the natural history of aortic atherosclerosis by TEE and finds no significant change in overall severity, but a high likelihood for individual lesions to worsen or regress. This supports the hypothesis that plaque turnover rates (i.e., rupture followed by

25   passivation) may be significant. TEMRI may, thus, have several potential advantages over TEE for monitoring plaque behavior. First, TEMRI allows imaging in any plane with precise registration to a fixed frame of reference. Since TEE requires manual aiming, the probe is not a fixed reference point, making TEE an imperfect tool for this purpose, particularly in areas with many plaques and few anatomic landmarks. Second,

30   TEMRI offers information about plaque composition which cannot be assessed as well by ultrasound-based techniques (e.g., Correia, L.C.L., et al.; Martin, A.J., et al., Radiographics, vol. 17, pp. 189-202; Yuan, C., et al., Arterioscler Thromb Vasc Biol., vol. 17, pp. 1496-503) and may predict plaque stability. It is believed that serial TEMRI

studies to monitor atherosclerotic plaques and their response to pharmacologic interventions may be beneficial.

In conclusion, TEMRI is superior to TEE in the quantification of atherosclerotic plaque extent in the thoracic aorta, and can be performed in combination with surface-coil MRI. Specifically, the TEMRI assessment of plaque extent is comprehensive since the entire circumference of the aorta can be visualized at any level and orientation as desired by the operator. Moreover, the relationship of individual plaques to structural landmarks is straightforward, making it ideal for follow-up studies given its minimally invasive nature and the lack of a need for sedation with its inherent risks and costs. Finally, the potential for detailed assessment of plaque composition in the near future makes TEMRI an important addition to cardiovascular medicine and clinical investigation.

Example 7

Figure 7 is a schematic diagram of another transesophageal magnetic resonance imaging device 82 which, except for receiver 84, is similar to the TEMRI device 70 of Figure 5C. A suitable TEMRI non-loopless antenna receiver 84, such as a coil, is connected via balun 72, TMD circuit 12 and coaxial cable 26 to the MRI scanner 18. Although the exemplary TEMRI antenna device 82 is not completely sealed at the antenna end 86, a sealed TEMRI device may also be employed. As is well known, the MRI scanner 18 may be employed for magnetic resonance imaging or spectroscopic analysis of the patient.

In addition to analysis of the aorta, it is believed that TEMRI may be employed with other intra thoracic anatomic structures to: (1) image and perform spectroscopy of the coronary arteries and study blood flow velocity, the presence, size and composition of atherosclerotic plaques, and the presence of coronary artery aneurysms; (2) study the heart muscle and perform imaging and spectroscopy of the heart in situations of health and disease; (3) image the valves of the heart to detect valve malfunctions such as stenoses and regurgitant jets; (4) image and perform spectroscopy in masses and/or tumors involving the heart or contained within the heart chambers; (5) image and perform spectroscopy of the pericardium in states of heath and disease; (6) image the pulmonary artery for the detection of congenital or acquired disease and to detect the presence of thrombus or tumor within the main pulmonary trunk and its branches; (7) image and perform spectroscopy of the mediastinum, lymph nodes and mediastinal masses; (8) image and perform spectroscopy of the lung tissues, lung tumors

or other pulmonary processes including pleural diseases and tumors; (9) image and perform spectroscopy of thoracic osseous and/or cartilagenous normal and pathologic structures including tumors or masses involving the thoracic bones and cartilages; and (10) image and perform spectroscopy of any of the above anatomic structures in combination with standard and/or modified surface coil imaging and spectroscopy.

In summary, TEMRI provides information about the aorta, which is of clinical importance, and which is otherwise unobtainable without invading a vascular space. TEMRI is further employed in visualizing lesions of the aorta.

The exemplary non-invasive method of imaging the thoracic aorta provides both morphological detail within the aortic wall as well as information about regional aortic wall motion. The exemplary TEMRI devices 2,70,82 allow transesophageal MR imaging of the thoracic aorta. This method has several advantages over the competing non-vasculoinvasive techniques of transesophageal echocardiography (TEE) or standard MRI. For example, use of the TEMRI devices 2,70,82 and TEMRI do not require a full invasive procedure and the associated sedatives. Furthermore, the thoracic aorta may be imaged in longitudinal and cross-sectional views, and details of the aortic wall being readily seen.

The TEMRI technique has direct application to studies of aortic atheroma size, morphology and composition. Those properties cannot be measured as well, or at all, by other known competing techniques. Non-invasive studies of, for example, changes in atherosclerotic plaques in response to pharmacologic interventions, may be considered using the TEMRI technique.

TEMRI also provides tissue tagging for measurement of focal stress/strain relationships. Furthermore, with the addition of ECG-gated cine tissue tagging, TEMRI offers the first known method of direct observation of regional stress/strain relationships in the aortic wall throughout the cardiac cycle.

Furthermore, TEMRI avoids the risks inherent in intravascular MRI, while providing comparable image quality.

Enhanced efficiency of TEMRI may be provided through the use of at least one of a balancing transformer and an impedance matching circuit.

While for clarity of disclosure reference has been made herein to an MRI scanner 18 for displaying an image, it will be appreciated that the image information may be stored, printed on hard copy, be computer modified, or be combined with other data. All

such processing shall be deemed to fall within the terms "display" or "displaying" as employed herein.

Whereas particular embodiments of the present invention have been described above for purposes of illustration, it will be appreciated by those skilled in the art that numerous variations in the details may be made without departing from the invention as described in the claims which are appended hereto.

WE CLAIM:

1.   A method of transesophageal magnetic resonance analysis of a patient having an esophagus and an intra thoracic anatomic structure, said method comprising:

providing a non-loopless antenna;

receiving said non-loopless antenna in a gastric tube;

inserting said gastric tube which receives said non-loopless antenna in the esophagus of said patient;

employing a matching and tuning circuit for said non-loopless antenna external to said patient;

electrically connecting said matching and tuning circuit to a magnetic resonance scanner; and

employing said magnetic resonance scanner for magnetic resonance imaging or spectroscopic analysis of the intra thoracic anatomic structure of said patient.

2.   The method of claim 1 including

employing as said intra thoracic anatomic structure an aorta.

3.   The method of claim 1 including

employing as said intra thoracic anatomic structure a structure selected from the list including: a heart tissue, a coronary artery, coronary blood, a coronary atherosclerotic plaque, a coronary artery aneurysm, a heart valve, a heart muscle, a heart tumor, a heart mass, a heart chamber, a pericardium, a pulmonary artery, a pulmonary thrombus, a pulmonary tumor, a mediastinum, a lymph node, a mediastinal mass, a lung tissue, a lung tumor, a thoracic tumor, a thoracic mass, a thoracic bone, and a thoracic cartilage.

4.   The method of claim 1 including

employing as said gastric tube a Levin gastric tube.

5.   The method of claim 1 including

employing as said gastric tube a nasogastric tube; and

employing transnasal placement of said nasogastric tube in the esophagus of said patient.

6.   The method of claim 1 including

employing as said gastric tube a gastric tube having an outer diameter of 8 French or 12 French.

7.   The method of claim 1 including

employing as said gastric tube a gastric tube having a diameter suitable for insertion in the esophagus of said patient.

8.   The method of claim 1 including

employing as said non-loopless antenna a receiver coil.

9.   The method of claim 1 including

adjusting said matching and tuning circuit.

10.   The method of claim 1 including

employing as said patient a non-sedated patient.

11.   The method of claim 1 including

employing as said patient a human being.

12.   The method of claim 1 including

employing as said patient an animal other than a human being.

13.   The method of claim 1 including

employing fluoroscopy to confirm proper placement of said gastric tube in the esophagus of said patient.

14.   The method of claim 1 including

employing said non-loopless antenna to confirm proper placement of said gastric tube in the esophagus of said patient.

15.   The method of claim 1 including

employing an image from an external body coil to confirm proper placement of said gastric tube in the esophagus of said patient.

16.   The method of claim 1 including

providing said gastric tube with visible markings; and

employing said visible markings of said gastric tube to facilitate proper placement thereof in the esophagus of said patient.

17.   The method of claim 16 including

measuring external to said patient a position for said proper placement of said gastric tube in said esophagus before marking said gastric tube with said visible markings; and

employing said visible markings to properly place said gastric tube in the esophagus of said patient.

18.   The method of claim 1 including

employing bias current to decouple said non-loopless antenna;

detecting a change in said bias current;

employing said magnetic resonance scanner to emit pulsed radio frequency signals; and

disabling said pulsed radio frequency signals in response to said change in said bias current.

19.   The method of claim 2 including

employing said aorta having an aortic wall;

employing blood within said aortic wall; and

displaying an image of said aortic wall and said blood.

20.   The method of claim 2 including

displaying an image of a longitudinal view of said aorta.

21.   The method of claim 2 including

displaying an image of a cross-sectional view of said aorta.

22.   The method of claim 1 including

employing tissue-tagging or ECG-gating to display an image of said structure.

23.   The method of claim 2 including

employing said aorta having a wall; and

demonstrating focal movement of the wall of said aorta in response to pulsatile blood flow which reflects focal stress/strain relationships.

24.   The method of claim 23 including

measuring said stress/strain relationships.

25.   The method of claim 2 including

employing said aorta having a wall; and

providing morphological detail within the wall of said aorta.

26.   The method of claim 2 including

employing said aorta having a wall; and

providing information about regional wall motion of said aorta.

27.   The method of claim 2 including

employing said aorta having a wall;

employing blood within the wall of said aorta;

employing tissues surrounding the wall of said aorta;

adjusting imaging parameters of said magnetic resonance scanner;

and

differentiating the wall of said aorta from said tissues and said

blood.

28.   The method of claim 2 including

displaying an image of said aorta; and

employing said image of said aorta to evaluate size, morphology, and composition of said aorta.

29.   The method of claim 2 including

employing said magnetic resonance scanner to emit pulsed radio frequency signals to said aorta and to receive magnetic resonance signals from said non-loopless antenna; and

employing diode switching in said matching and tuning circuit to decouple said non-loopless antenna during emission of said radio frequency pulses to said aorta, and to permit reception of said magnetic resonance signals between said radio frequency pulses.

30.   The method of claim 1 including

employing surface coil imaging and spectroscopy.

31.   A transesophageal magnetic resonance analysis apparatus for a patient having an esophagus and an intra thoracic anatomic structure, said apparatus comprising:

a non-loopless antenna;

a gastric tube for receiving said non-loopless antenna and for inserting said non-loopless antenna in the esophagus of said patient;

a matching and tuning circuit having a first port and a second port which is electrically connected to said non-loopless antenna;

magnetic resonance scanner means for magnetic resonance imaging or spectroscopic analysis of said intra thoracic anatomic structure of said patient; and

a cable electrically connecting the first port of said matching and tuning circuit to said magnetic resonance scanner means.

32.   The transesophageal magnetic resonance analysis apparatus of claim 31 including

said gastric tube is a Levin gastric tube.

33.   The transesophageal magnetic resonance analysis apparatus of claim 31 including

said gastric tube is a nasogastric tube for transnasal placement in the esophagus of said patient.

34.   The transesophageal magnetic resonance analysis apparatus of claim 31 including

said cable is a coaxial cable.

35.   The transesophageal magnetic resonance analysis apparatus of claim 31 including

said magnetic resonance scanner includes means for emitting pulsed radio frequency signals to said structure and means for receiving magnetic resonance signals from said non-loopless antenna; and

said matching and tuning circuit includes means for decoupling said non-loopless antenna during emission of said radio frequency pulses to said structure, and for permitting reception of said magnetic resonance signals between said radio frequency pulses.

36.   The transesophageal magnetic resonance analysis apparatus of claim 31 including

said non-loopless antenna is a receiver coil.

FIG. 1A

coax to MRI   TMD box   λ/4 coax   center conductor

housing   extension
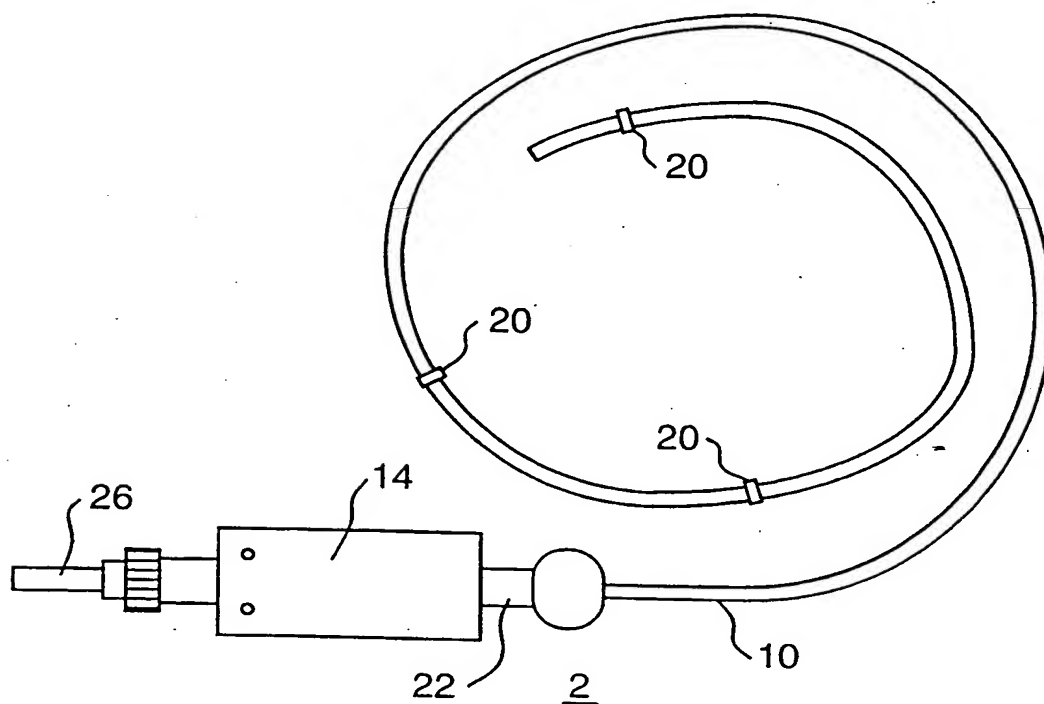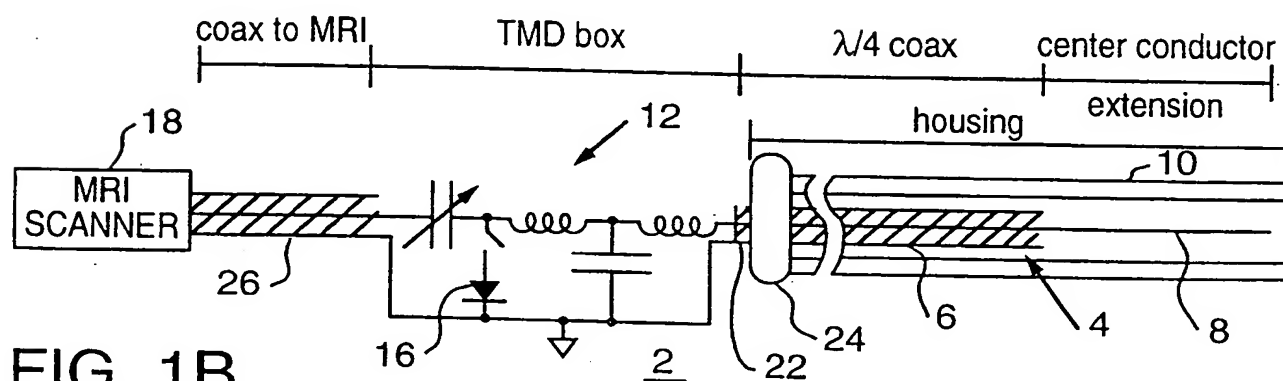
FIG. 1B
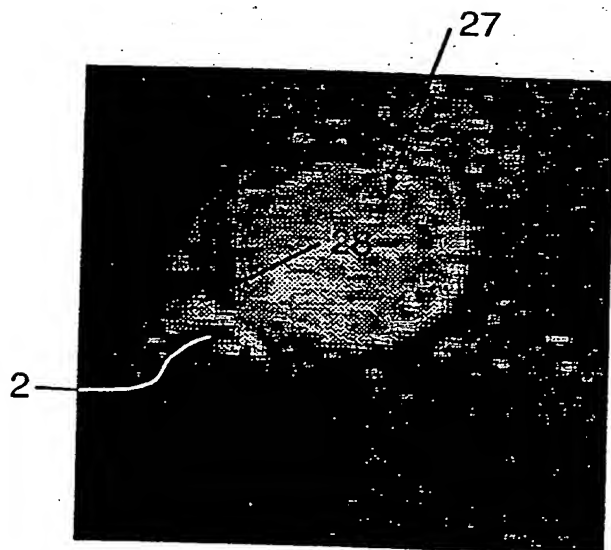
FIG. 2A
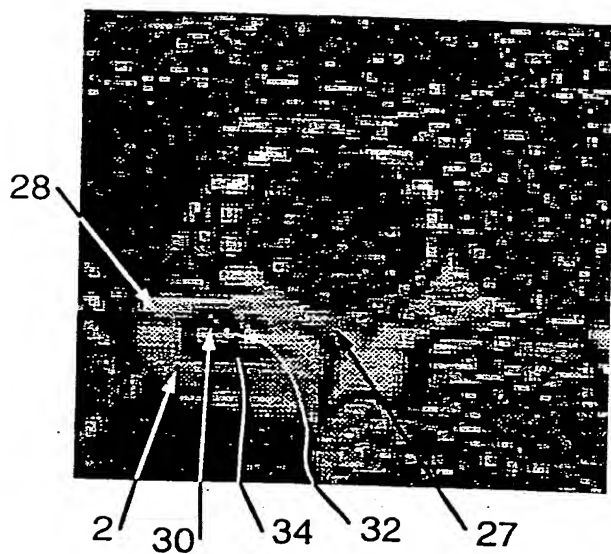
FIG. 2B
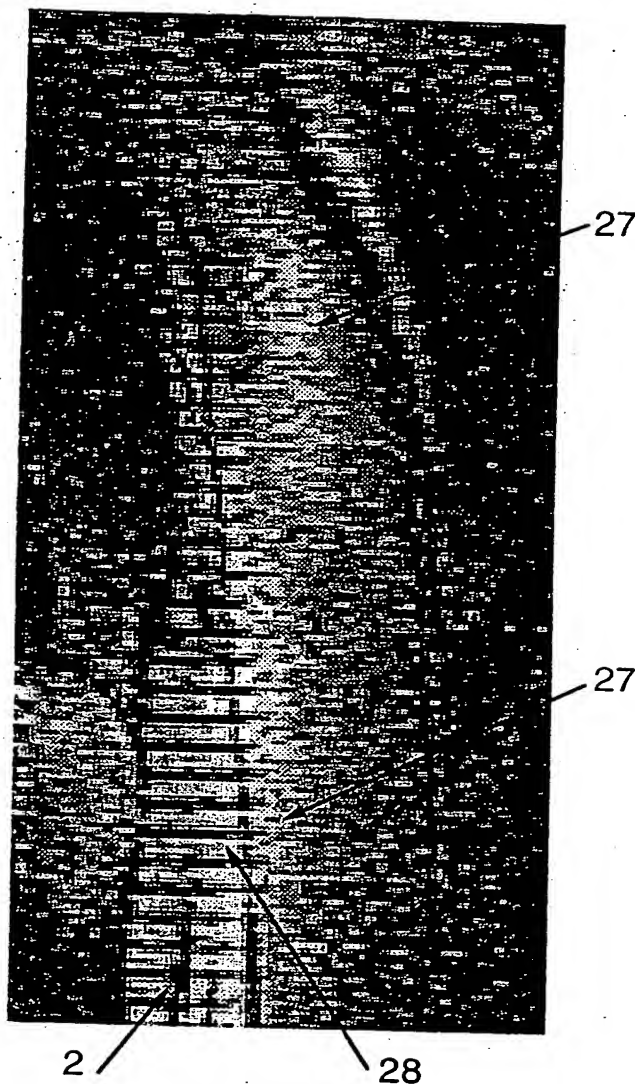
FIG. 2C

FIG. 3A
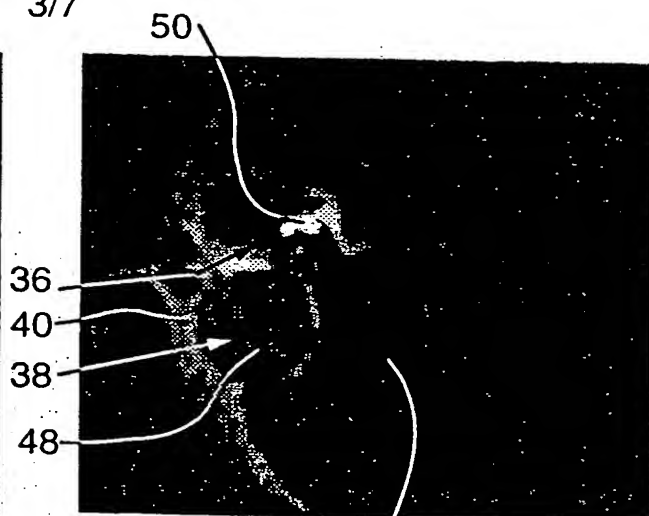
FIG. 3B
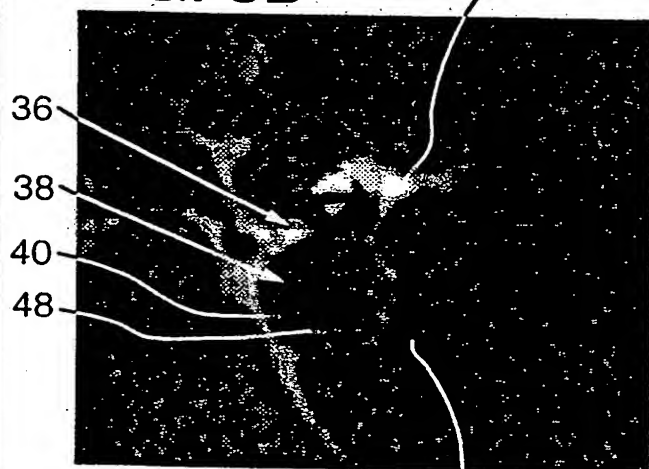
FIG. 3C
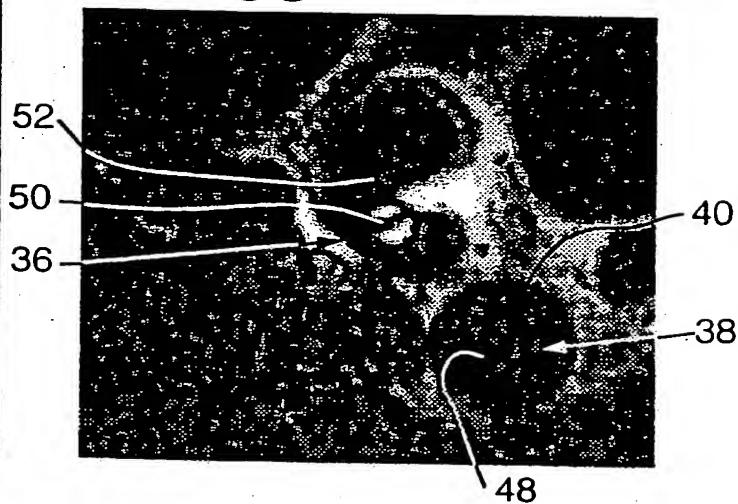
FIG. 3D
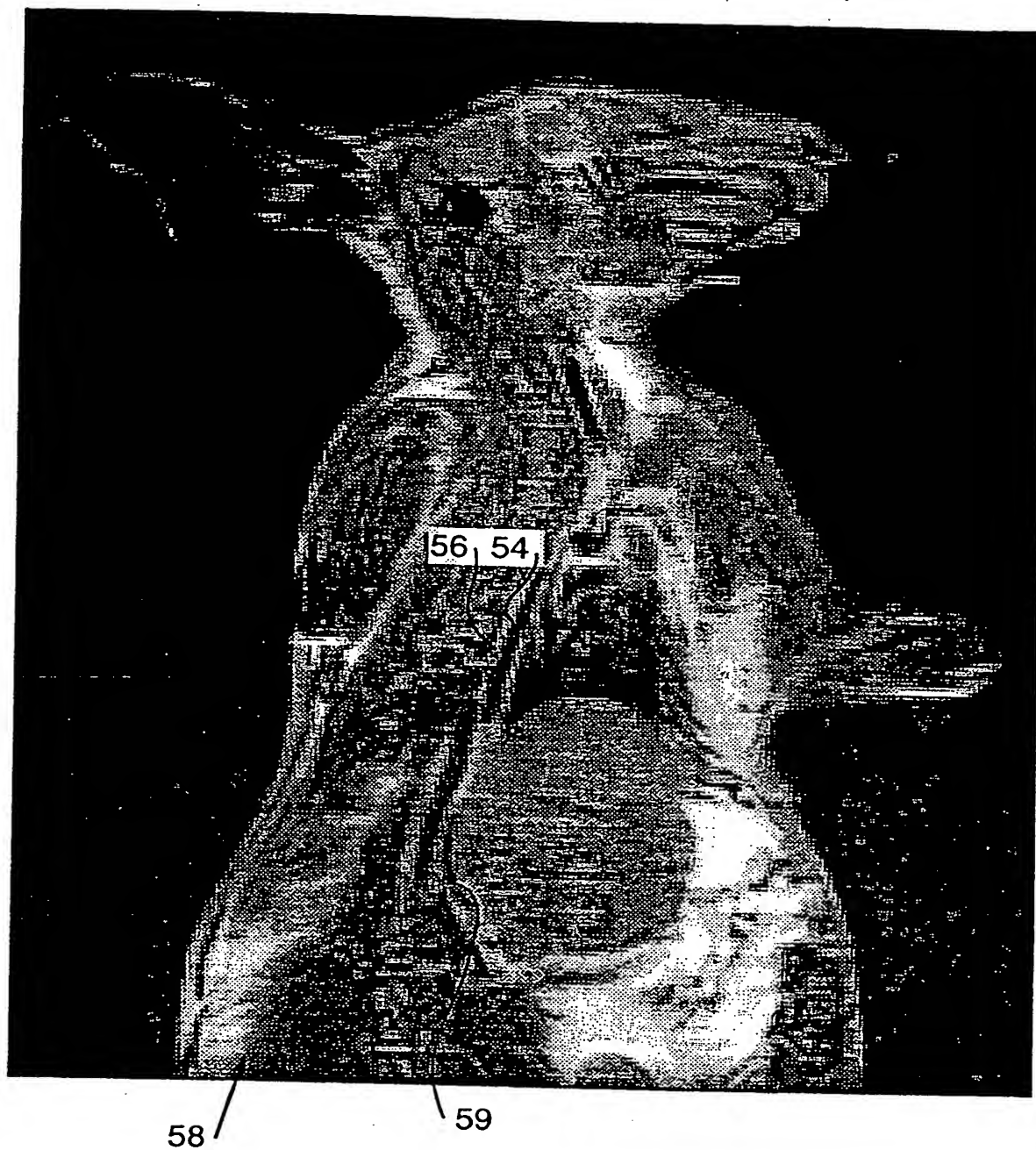
FIG. 4
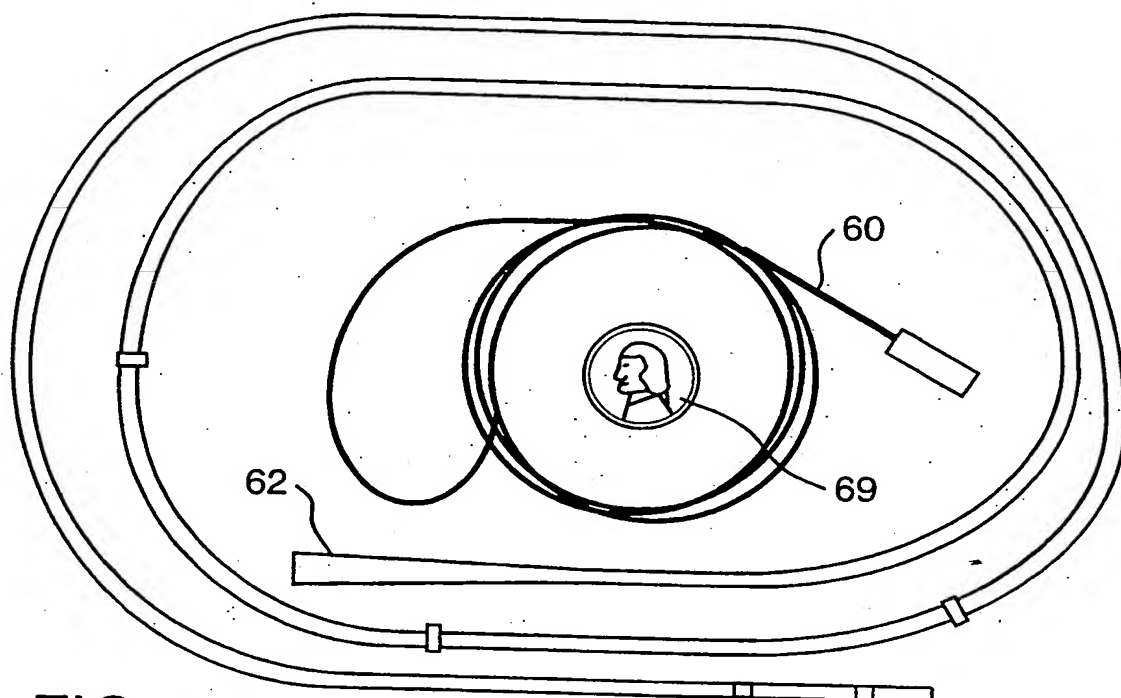
FIG. 5A
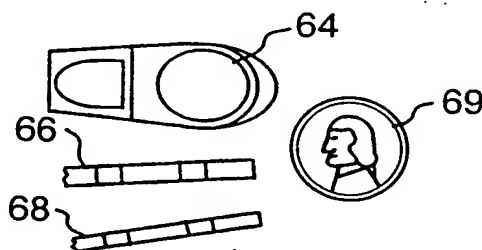
FIG. 5B Prior Art
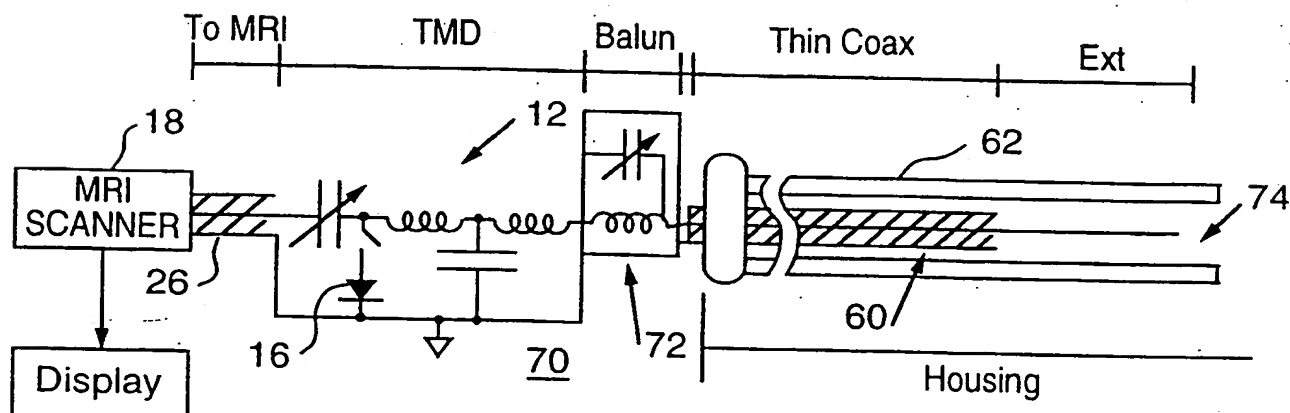
FIG. 5C
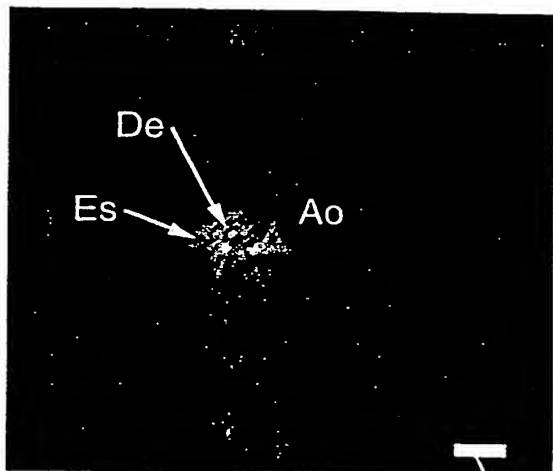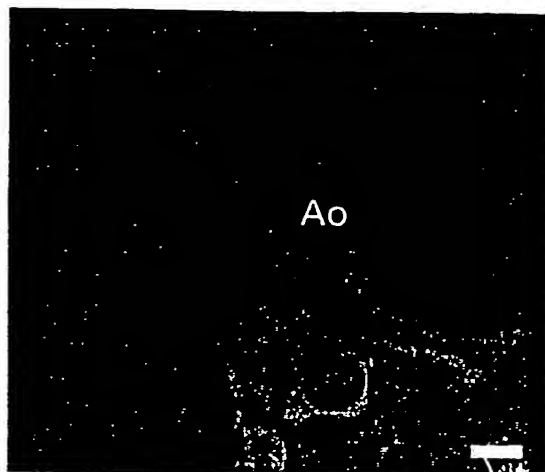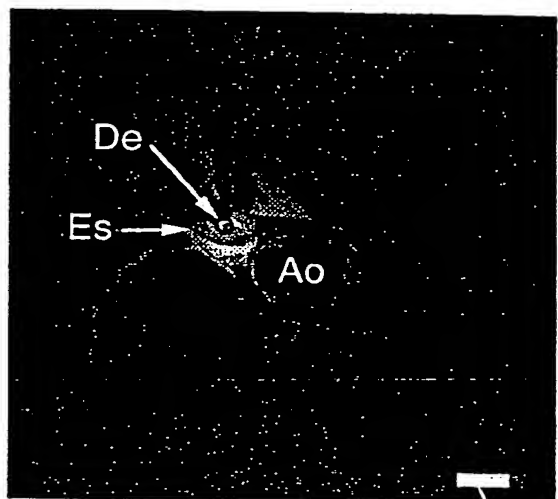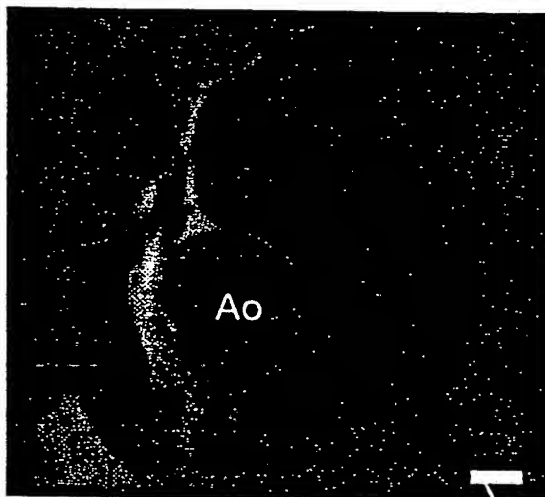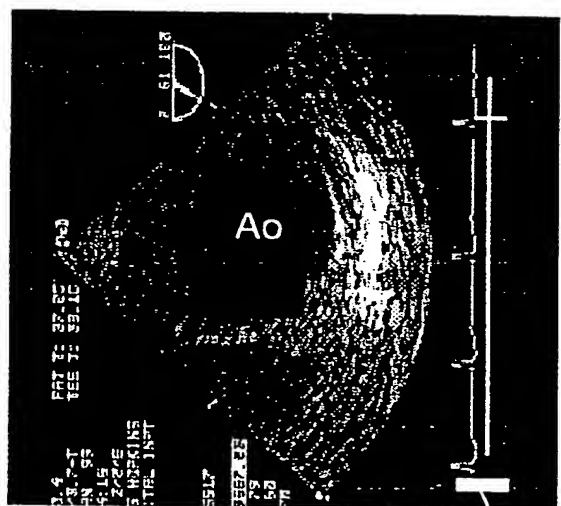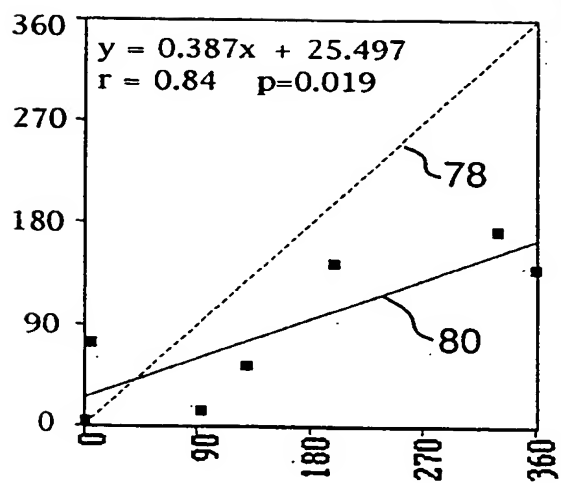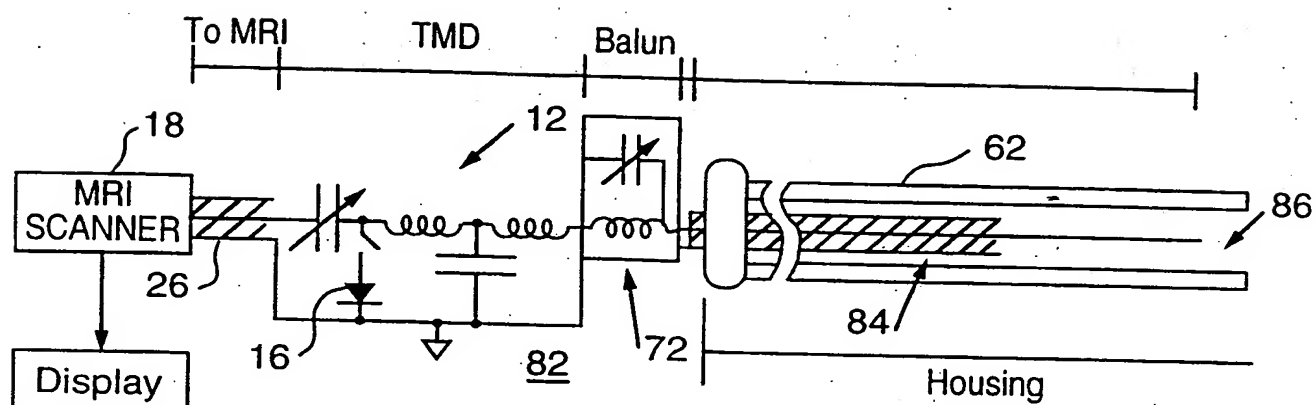
FIG. 6A

FIG. 6B


FIG. 6C

FIG. 6D

FIG. 6E

FIG. 6F

$y = 0.387x + 25.497$
$r = 0.84$ $p=0.019$

FIG. 7

INTERNATIONAL SEARCH REPORT

A. CLASSIFICATION OF SUBJECT MATTER
IPC(6) :A61B 5/055
US CL   :600/423
According to International Patent Classification (IPC) or to both national classification and IPC

B. FIELDS SEARCHED

Minimum documentation searched (classification system followed by classification symbols)
U.S. :   324/318, 322; 600/423

Documentation searched other than minimum documentation to the extent that such documents are included in the fields searched

Electronic data base consulted during the international search (name of data base and, where practicable, search terms used)

C. DOCUMENTS CONSIDERED TO BE RELEVANT

Category*	Citation of document, with indication, where appropriate, of the relevant passages	Relevant to claim No.
X	US 5,050,607 A (BRADLEY et al.) 24 September 1991, entire document.	1-36
X	US 5,355,087 A (CLAIBORNE et al.) 11 October 1994, entire document.	1-36
A	US 5,154,179 A (RATNER) 13 October 1992, col. 3 lines 35,36, col. 5 lines 23-25, 61-68, and col. lines 1-6.	1-7, 10-13, 16, 17, 31-33

☐ Further documents are listed in the continuation of Box C. ☐ See patent family annex.

* Special categories of cited documents:

"A" document defining the general state of the art which is not considered to be of particular relevance

"E" earlier document published on or after the international filing date

"L" document which may throw doubts on priority claim(s) or which is cited to establish the publication date of another citation or other special reason (as specified)

"O" document referring to an oral disclosure, use, exhibition or other means

"P" document published prior to the international filing date but later than the priority date claimed

"T" later document published after the international filing date or priority date and not in conflict with the application but cited to understand the principle or theory underlying the invention

"X" document of particular relevance: the claimed invention cannot be considered novel or cannot be considered to involve an inventive step when the document is taken alone

"Y" document of particular relevance: the claimed invention cannot be considered to involve an inventive step when the document is combined with one or more other such documents, such combination being obvious to a person skilled in the art

"&" document member of the same patent family

Date of the actual completion of the international search	Date of mailing of the international search report
10 FEBRUARY 2000	29 FEB 2000
Name and mailing address of the ISA/US Commissioner of Patents and Trademarks Box PCT Washington, D.C. 20231 Facsimile No. (703) 305-3230	Authorized officer RUTH S. SMITH Telephone No. (703) 308-3063

Form PCT/ISA/210 (second sheet)(July 1992)*